A Letters Journal Exploring the Frontiers of Physics

December 2019

EPL, **128** (2019) 58002 www.epljournal.org
doi: 10.1209/0295-5075/128/58002

Dual-band light-emitting diode based on microwheel cavity

Gangyi Zhu[1(a)], Mengyao Zhou[1], Siqing He[1], Feifei Qin[1], Boning Han[2], Yan Jiang[1], Xin Li[1], Haibo Zeng[2] and Yongjin Wang[1(b)]

[1] *College of Telecommunications and Information Engineering, Nanjing University of Posts and Telecommunications - Nanjing 210003, China*
[2] *MIIT Key Laboratory of Advanced Display Material and Devices, School of Materials Science and Engineering, Nanjing University of Science and Technology - Nanjing, 210094, China*

received 9 September 2019; accepted in final form 19 December 2019
published online 3 February 2020

PACS 85.60.Jb – Light-emitting devices
PACS 78.60.Fi – Electroluminescence
PACS 61.72.uj – III-V and II-VI semiconductors

Abstract – Compact and broadband electroluminescent (EL) devices have garnered considerable interest in recent years. In this study, we have fabricated a light-emitting diode (LED) based on a GaN microwheel cavity with a peak emission wavelength of 438 nm. Another emission peak at 512 nm is realized by coating $CH_3NH_3PbBr_3$ on the LED. The microwheel-cavity–based LED is fabricated by photolithography and inductively coupled plasma etching process. The opto-electrical performance of the device is characterized in terms of the EL spectrum, luminescence intensity, full width at half maximum, and 3 dB bandwidth. Compared to the device without the $CH_3NH_3PbBr_3$ layer, the proposed device exhibits dual-band illumination and higher 3 dB bandwidth with potential applications in optical communication.

Introduction. – Owing to their high luminous efficiency, long service life, and high integratibility, GaN-based light-emitting diodes (LEDs) have received considerable research attention in recent years [1–3]. Nowadays, high quality GaN-based LEDs are widely used as indicators, tail lights of vehicles, decorated lamps, backlights of displays, and lighting [4–7]. As it is quite easy to fabricate GaN-based blue LEDs, extending the emission region of such LEDs and improving their optical performance is of great significance. The resonant-cavity LED (RCLED) is a promising candidate to obtain high-performance devices with improved light emission because the active region is placed inside a resonant cavity in these LEDs, and therefore the optical emission is restricted to the cavity modes [8,9]. The nanostructure formed on a photonic crystal (PhC) and the microstructure formed on a patterned sapphire substrate provide relatively uniform structures for the fabrication of such LEDs [10,11].

Currently, sapphire, SiC, and Si are mainly used as substrates for GaN-based devices. Due to the low cost, large size, low resistivity, and high thermal conductivity, Si has emerged as the prevalent substrate among them. Further, compared to the other methods, photoetching is an established technique to fabricate the micro/nanostructure of GaN-based materials, which improves the efficiency of LEDs [12–14]. On the other hand, normal white LEDs can emit light by several methods [15–17]. For example, existing colored LEDs with red, green, and blue chips comprise two structures: one is to enclose a chip that emits light of each color into a light-diffusing material, and the other is to enclose each chip in a resin. Each chip has its own lens in the light-diffusing material. Based on the idea of light diffusion, we combined a blue GaN LED and the $CH_3NH_3PbBr_3$ material, which has higher quantum efficiency and brightness in the green region [18–20], to design a multi-emission structure with GaN microwheel and $CH_3NH_3PbBr_3$ coating layer. As $CH_3NH_3PbBr_3$ emits green light at 520 nm and the GaN LED emits near 438 nm, it is easy to realize the excitation of $CH_3NH_3PbBr_3$ in the hybrid structure, thereby extending the emission region of the device.

In this study, we fabricated the GaN microwheel cavity by photolithography and inductively coupled plasma (ICP) etching of III-V materials. For achieving dual-band illumination, we vaporized a $CH_3NH_3PbBr_3$ layer on the microwheel cavity. The opto-electrical performance of the

(a) E-mail: zhugangyi@njupt.edu.cn
(b) E-mail: wangyj@njupt.edu.cn

device was analysed in terms of the electroluminescent (EL) spectrum, luminescence intensity, full width at half maximum, and 3 dB bandwidth.

Experimental section. –

Device fabrication. The GaN-microwheel–based LED was fabricated using a GaN-on-silicon wafer. The wafer consisted of a GaN layer and silicon substrate with a thickness of 4.5 and 1600 μm, respectively. The GaN layer included a p-GaN layer (115 nm), InAlGaN quantum wells (13 nm), n-GaN layer (3400 nm), and u-GaN layer (1000 nm). A schematic of the fabrication process for the GaN-microwheel–based LED is illustrated in fig. 1. Firstly, the photoresist layer is patterned by photolithography (step (a)), and then a 200 nm nickel film is deposited as a hard mask by thermal evaporation (step (b)). After removing the residual photoresist, the top surface of the wafer is etched down to the silicon layer with a depth of 4.5 μm by ICP etching. The parameters of ICP etching are as follows: chlorine flow rate = 40 sccm, boron trichloride flow rate = 4 sccm, power = 300 W, pressure = 4 mTorr, time = 8 minutes, etching rate of GaN ~0.575 μm/min, and etching thickness of GaN ~4.5 μm. After removing the residual nickel film by diluting the wafer in nitric acid (step (c)), the photoresist layer is patterned by photolithography (step (d)), and then a 200 nm nickel film is deposited as a hard mask by thermal evaporation (step (e)). After removing the residual photoresist, the wafer is etched down to the n-GaN layer by ICP etching, and then the residual nickel film is removed by diluting the wafer in nitric acid (step (f)). After the photoresist layer is patterned by photolithography (step (g)), Au/Ni films are deposited on the surface of GaN as p/n electrode and then the residual photoresist is removed (step (h)). Finally, we evaporate the $CH_3NH_3PbBr_3$ layer on the surface of GaN microcavity (step (i)). The $CH_3NH_3PbBr_3$ layer was fabricated using the two-step vacuum thermal evaporation deposition technique. During this experiment, $PbBr_2$ powder was placed in a ceramic crucible, and the GaN microwheel device was placed face-down above the crucible at a height of ~15 cm. The pressure was increased to 3×10^{-4} Pa. The deposition rate and film thickness were monitored by a quartz crystal. The $PbBr_2$ film was deposited at the rate of 1 nm s^{-1}. The CH_3NH_3Br film was fabricated by the same method and condition. Finally, the prepared sample was placed in a glove box to protect it against moisture and oxygen for 24 h.

Figure 2(a) shows the scanning electron microscopy (SEM) image of a GaN microwheel (Hitachi SU-8010), where its diameter is observed as 100 μm. It is clear that the top surface of the GaN microwheel is smooth. Figure 2(b) shows the optical image of the device with an Au electrode. As shown in fig. 2(c), the diffraction peaks near 15.16°, 21.37°, and 30.3° corresponding to the (001), (011), and (002) lattice planes of the cubic structure, respectively, are consistent with a single

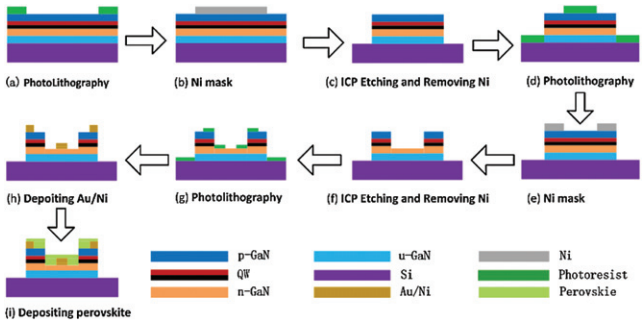

Fig. 1: Schematic for the fabrication process of GaN microwheel with perovskite layer.

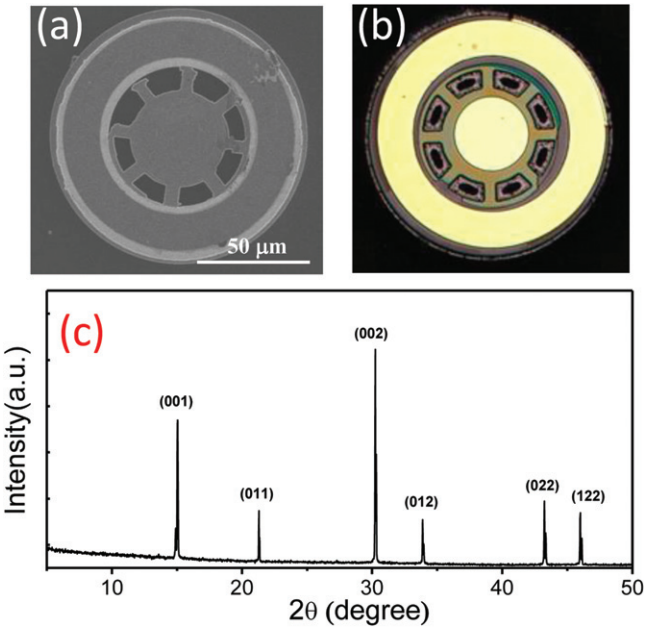

Fig. 2: (a) SEM image of a GaN microwheel. (b) Optical image of a GaN microwheel. (c) XRD pattern of the $CH_3NH_3PbBr_3$ film.

crystal of $CH_3NH_3PbBr_3$ grown at room temperature. The structure of the GaN microwheel cavity can be set as RCLED. The PL spectra of this cavity and of the $CH_3NH_3PbBr_3$ coating layer were measured with a micro photoluminescence (μ-PL) system. During this experiment, a Nd:YAG pulsed laser (355 nm, 10 Hz, 6 ns) was employed as the excitation light source. The EL spectra of the devices were obtained with a micro probe system integrated with an alternating current source and fiber coupled spectrograph.

Results and discussion. – Figure 3 shows the current dependent EL spectra of different devices. It is evident from fig. 3(a) that the pure microwheel structure has an emission peak at 438 nm when the current is 0.5 mA. As the current increases, the output intensity increases, but the emission wavelength remains unchanged. After coating $CH_3NH_3PbBr_3$ (fig. 3(b)), the turn-on current of the device increases to 1.5 mA. When the current is above 1.5 mA, two clear peaks are observed at 438 nm

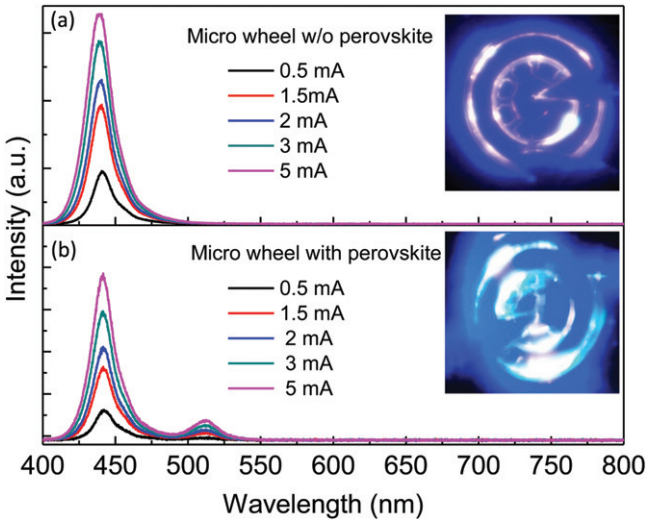

Fig. 3: EL spectrum of a GaN microwheel (a) without $CH_3NH_3PbBr_3$ and (b) with $CH_3NH_3PbBr_3$ for varying current.

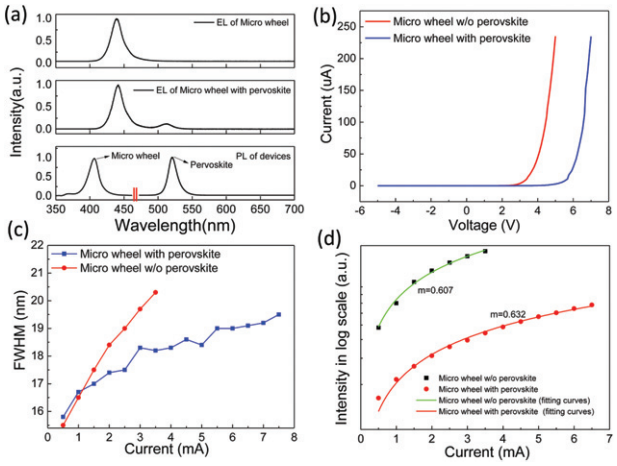

Fig. 4: (a) EL spectra of GaN microwheel and $CH_3NH_3PbBr_3$ decorated structure, and PL spectra of GaN microwheel and $CH_3NH_3PbBr_3$. (b) I-V curves, (c) FWHM and (d) peak intensity *vs.* current of GaN microwheel in the presence and absence of $CH_3NH_3PbBr_3$. The solid lines in (d) represent power-law exponent fitting.

and 512 nm with full width at half maximum (FWHM) of 17.5 nm and 17 nm, respectively. As the current increases, the output intensity gradually increases but the position of the peaks remains stable. The dual-band emission can be attributed to the fact that the blue emission of GaN LED can stimulate the PL of $CH_3NH_3PbBr_3$. The insets in fig. 3 show the images of the devices obtained by a charge coupled device (CCD) camera using an electrically pumped laser. As expected, the chromaticity of the device is changed to the visible region.

The inset images show the CCD image of each structure. To further understand the properties of the devices, their EL and PL spectra are shown in fig. 4(a). It is evident that the GaN microwheel emits in the blue region while the $CH_3NH_3PbBr_3$ decorated structure has a second peak in the green region. This observation is further confirmed in the PL spectra of GaN and $CH_3NH_3PbBr_3$, which show ultraviolet light emission near 407 nm and green light emission near 520 nm. Figure 4(b) displays the current-voltage (I-V) curves of the GaN microwheel with and without the $CH_3NH_3PbBr_3$ coating. The turn-on voltage of the GaN microwheel with and without $CH_3NH_3PbBr_3$ is 6 V and 2.5 V, respectively. This result is consistent with the inference drawn from fig. 3 that it is more difficult to turn on the perovskite covered sample. The increase in the turn-on voltage may be attributed to the fact that the carrier transfer rate is decreased by the $CH_3NH_3PbBr_3$ layer. Figure 4(c) shows the FWHM of GaN microwheel *vs.* current for different structures. As the current increases, the FWHM is also increased. Besides, the FWHM of GaN microwheel with $CH_3NH_3PbBr_3$ is lower than that of the sample without $CH_3NH_3PbBr_3$ under the same current. This is because the $CH_3NH_3PbBr_3$ coating decreases the carrier concentration of the device. For the GaN microwheel with $CH_3NH_3PbBr_3$, the intensity of the emitted light (peak intensity) and the FWHM are decreased, and the electrical characteristics are degraded when dual-band illumination is achieved. Figure 4(d) shows the variation of peak intensity as a function of current for GaN microwheel with and without $CH_3NH_3PbBr_3$. As the current increases, the peak intensity increases as well. The peak intensity of the GaN microwheel without $CH_3NH_3PbBr_3$ is larger than that of the GaN microwheel with $CH_3NH_3PbBr_3$ at the same current. This is because most of the blue emitted light is absorbed by the $CH_3NH_3PbBr_3$ layer, as is clear from the PL spectra in fig. 4(a). For a normal LED, the output EL intensity is proportional to I_0^m, where I_0 is the injected current [21], and $m = 1$ and 2 if the emission corresponds to the diffusion current and recombination current, respectively. According to the power-law fitting in fig. 4(d), $m \sim 0.6$ in both the devices. This low value of m indicates that most of the emission may not contribute to the EL of the devices.

Figures 5(a) and (b) show the 3 dB bandwidth of the GaN microwheel with and without $CH_3NH_3PbBr_3$, respectively. It is clear that the bandwidth increases with the bias voltage and is higher near 6–8 V. The 3 dB bandwidths of the GaN microwheel with and without $CH_3NH_3PbBr_3$ are highest at 6 V, and are 16 MHz and 14 MHz, respectively. Comparing the two figures, figs. 3(a) and (b), it can be seen that the overall amplitude of the LED with perovskite is reduced, indicating that the addition of perovskite will reduce the overall brightness. However, this decrease in brightness is not flat in the frequency domain. Specifically, the amplitude of the low-frequency component of the perovskite LED decreases more and the amplitude of the high-frequency portion decreases less than that of the ordinary LED. This feature results in a 3 dB bandwidth for the LED with perovskite that is larger than that of a normal LED. Figure 5(c) summarizes

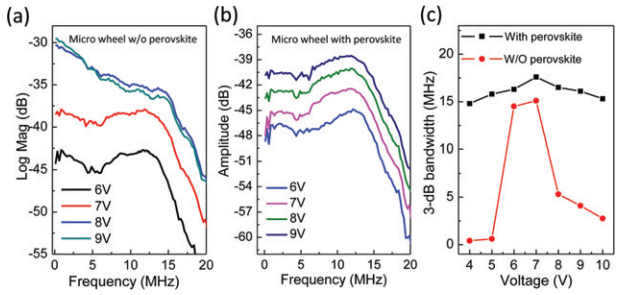

Fig. 5: 3 dB bandwidth of GaN microwheel (a) without $CH_3NH_3PbBr_3$ and (b) with $CH_3NH_3PbBr_3$ for varying voltage; (c) 3 dB bandwidth of different devices *vs.* voltage.

the bandwidth at each voltage, which indicates that the $CH_3NH_3PbBr_3$-coated sample has a larger 3 dB bandwidth. This facilitates the suitability of the combined structure for communication applications. Figure 5(c) also demonstrates that the combined sample is less sensitive to the voltage, *i.e.*, the trend of 3 dB bandwidth curve remains relatively flat as the voltage increases. On the contrary, when the voltage exceeds 7 V, the 3 dB bandwidth of the GaN microwheel without $CH_3NH_3PbBr_3$ is significantly reduced.

Conclusions. – We fabricated a dual-band GaN-microwheel–based LED with a $CH_3NH_3PbBr_3$ coating layer. The GaN microwheel was prepared by photolithography and ICP etching. The dual-band illumination of the device was validated by the *I-V* curves, EL intensity, and the corresponding FWHM. This device exhibited two emission peaks near 438 nm and 512 nm. Further, the 3 dB bandwidth measurement indicated a 16 MHz bandwidth at 6 V for the combined structure, which is much higher and stable than that of the uncoated one. The extension of the emission region and improvement in the communication ability of the proposed device provides a potential approach for the realization of full color LEDs or broadband communication in future.

* * *

This work is jointly supported by Jiangsu Province Outstanding Youth Fund (BK20180087), the China Postdoctoral Science Foundation (2018M630588), Peaks Project in Jiangsu Province (DZXX-018).

REFERENCES

[1] Dadgar A., Hums C., Diez A., Blaesing J. and Krost A., *J. Cryst. Growth*, **297** (2006) 279.
[2] Koide N., Kato H., Sassa M., Yamasaki S., Manabe K., Hashimoto M., Amano H., Hiramatsu K. and Akasaki I., *J. Cryst. Growth*, **115** (1991) 639.
[3] Hwang D. K., Kang S. H., Lim J. H., Yang E. J., Oh J. Y., Yang J. H. and Park S. J., *Appl. Phys. Lett.*, **86** (2005) 222101.
[4] Kim T.-H., Cho K.-S., Lee E. K., Lee S. J., Chae J., Kim J. W., Kim D. H., Kwon J.-Y., Amaratunga G., Lee S. Y., Choi B. L., Kuk Y., Kim J. M. and Kim K., *Nat. Photonics*, **5** (2011) 176.
[5] Han H.-V., Lin H.-Y., Lin C.-C., Chong W.-C., Li J.-R., Chen K.-J., Yu P., Chen T.-M., Chen H.-M., Lau K.-M. and Kuo H.-C., *Opt. Express*, **23** (2015) 32504.
[6] Meneghini M., Tazzoli A., Mura G., Meneghesso G. and Zanoni E., *IEEE Trans. Electron Devices*, **57** (2010) 108.
[7] Li G., Wang W., Yang W., Lin Y., Wang H., Lin Z. and Zhou S., *Rep. Prog. Phys.*, **79** (2016) 056501.
[8] Schubert E. F., Wang Y. H., Cho A. Y., Tu L. W. and Zydzik G. J., *Appl. Phys. Lett.*, **60** (1992) 921.
[9] Cai W., Yuan J., Ni S., Shi Z., Zhou W., Liu Y., Wang Y. and Amano H., *Appl. Phys. Express*, **12** (2019) 032004.
[10] Matsubara H., Yoshimoto S., Saito H., Jianglin Y., Tanaka Y. and Noda S., *Science*, **319** (2008) 445.
[11] Lee T.-X., Gao K.-F., Chien W.-T. and Sun C.-C., *Opt. Express*, **15** (2007) 6670.
[12] Chang T.-L., Chen Z.-C. and Lee Y.-C., *Opt. Express*, **20** (2012) 15997.
[13] Zhang H., Zhu J., Zhu Z., Jin Y., Li Q. and Jin G., *Opt. Express*, **21** (2013) 13492.
[14] Jeong H., Kim Y. H., Seo T. H., Lee H. S., Kim J. S., Suh E.-K. and Jeong M. S., *Opt. Express*, **20** (2012) 10597.
[15] Sheu J. K., Chang S. J., Kuo C. H., Su Y. K., Wu L. W., Lin Y. C., Lai W. C., Tsai J. M., Chi G. C. and Wu R. K., *IEEE Photon. Technol. Lett.*, **15** (2003) 18.
[16] Sheu J. K., Pan C. J., Chi G. C., Kuo C. H., Wu L. W., Chen C. H., Chang S. J. and Su Y. K., *IEEE Photonics Technol. Lett.*, **14** (2002) 450.
[17] Hide F., Kozodoy P., DenBaars S. P. and Heeger A. J., *Appl. Phys. Lett.*, **70** (1997) 2664.
[18] Schmidt L. C., Pertegás A., González-Carrero S., Malinkiewicz O., Agouram S., Mínguez Espallargas G., Bolink H. J., Galian R. E. and Pérez-Prieto J., *J. Am. Chem. Soc.*, **136** (2014) 850.
[19] Tanaka K., Takahashi T., Ban T., Kondo T., Uchida K. and Miura N., *Solid State Commun.*, **127** (2003) 619.
[20] Huang H., Susha A. S., Kershaw S. V., Hung T. F. and Rogach A. L., *Adv. Sci.*, **2** (2015) 1500194.
[21] Nakamura S., Mukai T. and Senoh M., *Jpn. J. Appl. Phys.*, **30** (1991) L1998.